











## PERSPECTIVE

# Centiloid recommendations for clinical context-of-use from the AMYPAD consortium

Lyduine E. Collij<sup>1,2,3</sup>  | Ariane Bollack<sup>4,5</sup>  | Renaud La Joie<sup>6</sup>  |  
 Mahnaz Shekari<sup>7,8,9</sup>  | Santiago Bullich<sup>10</sup> | Núria Roé-Vellvé<sup>10</sup> | Norman Koglin<sup>10</sup>  |  
 Aleksandar Jovalekic<sup>10</sup> | David Valléz García<sup>1,2</sup>  | Alexander Drzezga<sup>11,12,13</sup> |  
 Valentina Garibotto<sup>14,15,16</sup>  | Andrew W. Stephens<sup>10</sup>  | Mark Battle<sup>4</sup> |  
 Christopher Buckley<sup>4</sup> | Frederik Barkhof<sup>1,2,5,17</sup>  | Gill Farrar<sup>4</sup> |  
 Juan Domingo Gispert<sup>7,8,9,18</sup>  | On behalf of the AMYPAD consortium

<sup>1</sup>Department of Radiology & Nuclear Medicine, Amsterdam UMC, Vrije Universiteit, Amsterdam, The Netherlands

<sup>2</sup>Brain Imaging, Amsterdam Neuroscience, Amsterdam, The Netherlands

<sup>3</sup>Clinical Memory Research Unit, Department of Clinical Sciences Malmö, Faculty of Medicine, Lund University, Malmö, Sweden

<sup>4</sup>GE Healthcare, Chalfont St Giles, Buckinghamshire, UK

<sup>5</sup>Centre for Medical Image Computing, University College London, London, UK

<sup>6</sup>Memory and Aging Center, Department of Neurology, University of California, San Francisco, California, USA

<sup>7</sup>Barcelonaβeta Brain Research Center, Pasqual Maragall Foundation, Wellington, Barcelona, Spain

<sup>8</sup>IMIM (Hospital del Mar Medical Research Institute), Barcelona, Spain

<sup>9</sup>Universitat Pompeu Fabra, Barcelona, Spain

<sup>10</sup>Life Molecular Imaging GmbH, Berlin, Germany

<sup>11</sup>Department of Nuclear Medicine, Faculty of Medicine and University Hospital Cologne, University of Cologne, Cologne, Germany

<sup>12</sup>German Center for Neurodegenerative Diseases (DZNE), Bonn, Germany

<sup>13</sup>Institute of Neuroscience and Medicine (INM-2), Molecular Organization of the Brain, Forschungszentrum, Jülich, Germany

<sup>14</sup>Division of Nuclear Medicine and Molecular Imaging, University Hospitals of Geneva, Geneva, Switzerland

<sup>15</sup>Department of Radiology and Medical Informatics, University of Geneva, Geneva, Switzerland

<sup>16</sup>CIBM Center for Biomedical Imaging, Lausanne, Switzerland

<sup>17</sup>Queen Square Institute of Neurology, University College London, London, UK

<sup>18</sup>CIBER Bioingeniería, Biomateriales y Nanomedicina (CIBER-BBN), Madrid, Spain

**Correspondence**

Lyduine E. Collij, Radiology and Nuclear Medicine PK -1x014, Amsterdam UMC, Location VUmc, Boelelaan 1117, 1081 HV Amsterdam, Netherlands.  
Email: l.collij@amsterdamumc.nl

**Abstract**

Amyloid-PET quantification through the tracer-independent Centiloid (CL) scale has emerged as an essential tool for the accurate measurement of amyloid- $\beta$  ( $A\beta$ ) pathology in Alzheimer's disease (AD) patients. The AMYPAD consortium set out to integrate existing literature and recent work from the consortium to provide clinical

Lyduine E. Collij and Ariane Bollack contributed equally to this study.

This is an open access article under the terms of the [Creative Commons Attribution](https://creativecommons.org/licenses/by/4.0/) License, which permits use, distribution and reproduction in any medium, provided the original work is properly cited.

© 2024 The Author(s). *Alzheimer's & Dementia* published by Wiley Periodicals LLC on behalf of Alzheimer's Association.

**Funding information**

Innovative Medicines Initiative 2 Joint Undertaking, Grant/Award Number: 115952; European Union's Horizon 2020; EFPIA; Innovative Medicines Initiative, Grant/Award Number: 115952

context-of-use recommendations for the CL scale. Compared to histopathology, visual reads, and cerebrospinal fluid, CL quantification accurately reflects the amount of AD pathology. With high certainty, a CL value below 10 excludes the presence of A $\beta$  pathology, while a value above 30 corresponds well with pathological amounts. Values falling in between these two cutoffs ("intermediate range") are related to an increased risk of disease progression. Together, CL quantification is a valuable adjunct to visual assessments of amyloid-PET images. An abnormal amyloid biomarker assessment is a key criterion to determine eligibility for anti-amyloid disease-modifying therapies, and amyloid-PET quantification can add further value by precisely monitoring amyloid clearance, and hence guiding patient management decisions.

**KEYWORDS**

Amyloid- $\beta$ , Centiloid quantification, clinical trials, positron emission tomography

**Highlights**

- Centiloid (CL) quantification robustly reflects of the amount of A $\beta$  pathology.
- CL < 10/CL > 30 reflects A $\beta$ -negativity/positivity thresholds with high certainty.
- CL quantification is a valuable adjunct to visual assessments of amyloid-PET.
- CL quantification can support trial design and treatment management.
- CL quantification could support the identification of early or emerging A $\beta$  pathology.

**1 | INTRODUCTION**

Biomarker quantification has emerged as a pivotal tool in the management of various diseases, allowing for precise measurements of critical parameters for clinical decision-making and the development of novel drugs. In Alzheimer's disease (AD), the ability to quantify its primary pathological hallmark amyloid- $\beta$  (A $\beta$ ) through amyloid positron emission tomography (PET) imaging is a central tool for improving diagnostic accuracy and patient management.<sup>1-3</sup> The emerging era of anti-amyloid therapies investigated monoclonal antibodies such as aducanumab,<sup>4</sup> gantenerumab,<sup>5</sup> lecanemab<sup>6,7</sup> and donanemab,<sup>8</sup> and relied on amyloid-PET for patient selection, evaluation of target-engagement, and assessment of drug effectiveness. In the Phase-III study of donanemab, amyloid-PET quantification was additionally utilized for making end-of-treatment decisions. Therefore, this imaging technique serves as a key biomarker guiding therapeutic strategies and could become an integrated part of clinical routine.

Until recently, the most common amyloid-PET metric was the standardized uptake value ratio (SUVr) with thresholds specific to each tracer and processing pipeline. The Centiloid (CL) approach provides a universal means of calibrating SUVr measures of A $\beta$  deposits into a tracer and quantification method-independent unbounded scale.<sup>9</sup> This quantification in "absolute" units can be leveraged into the definition of thresholds differentiating stages of AD pathology.<sup>10-16</sup> However, considering the abundance of literature regarding CL cutoffs, disease stages, and their utility, there is a need for a structured and detailed overview to further the interpretability of the CL metric along the AD continuum and its clinical use. This work aimed to analyze and integrate

the available knowledge of CL quantification and provide context-of-use recommendations for the implementation of the CL scale in clinical practice. These efforts have been collected and submitted as an application for a Biomarker Qualification Opinion (BQO) to the European Medicines Agency (EMA) on behalf of the Amyloid Imaging to Prevent AD (AMYPAD) consortium ([www.amypad.eu](http://www.amypad.eu)). A draft opinion was adopted by the Committee for Medicinal Products for Human Use (CHMP) and published (EMADOC-1700519818-1200791).

**2 | THE CENTILOID SCALE: DEFINITION AND PROCESSING**

Amyloid-PET quantification is commonly performed by normalizing the PET signal in a target region-of-interest (ROI) by the PET signal in a reference ROI supposedly free of specific tracer binding and summarized in the SUVr metric. Across the three regulatory approved radiotracers ([<sup>18</sup>F]florbetapir,<sup>17</sup> [<sup>18</sup>F]florbetaben,<sup>18</sup> [<sup>18</sup>F]flutemetamol<sup>19</sup>), differences in tracer binding and variability in image processing methodologies amplified in multi-center studies led to the conceptualization of the tracer-independent CL scale.<sup>9</sup> More specifically, the CL method allows the transformation of amyloid PET data acquired at individual sites using the individual settings and processing into standard CL units using a two-step scaling process. The key principle involves calibrating the SUVr of 18F-labeled tracers to match those of [<sup>11</sup>C]Pittsburgh compound B (PiB), which are then transformed into the CL scale. The scale is anchored to the mean amyloid load of a reference young healthy control group (CL = 0) and to the mean amyloid load of a

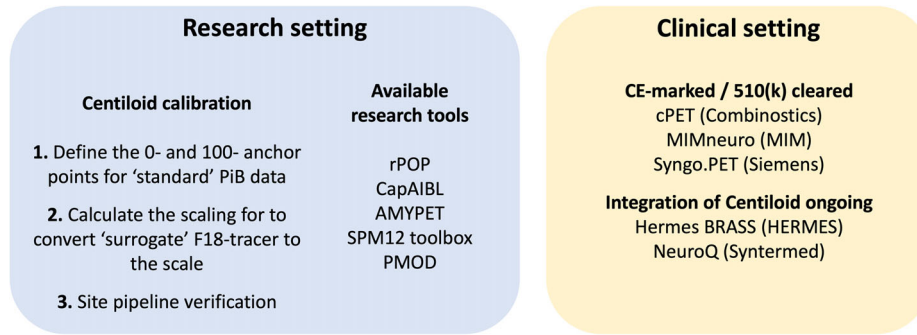


**FIGURE 1** Overview of Centiloid implementation and available software in research and clinical settings. PiB, Pittsburgh compound B.

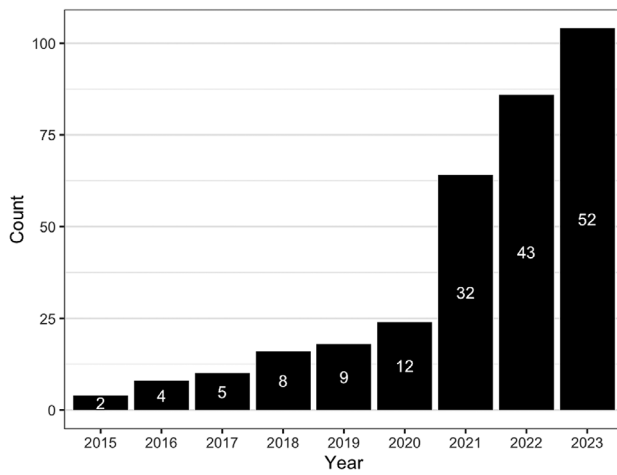


**FIGURE 2** Centiloid publications in PubMed (search performed on the 01/01/24).

typical mild-moderate AD population (CL = 100), available through the open-source Global Alzheimer's Association Interactive Network (GAAIN) reference dataset (<https://gaain.org/centiloid-project>), but values may be below 0 and above 100. The local processing pipeline is validated using specific quantitative criteria against the open-source GAAIN dataset. Importantly, these calibration steps should be performed according to the guidelines mentioned in Klunk et al.<sup>9</sup> for scientific use. For further clinical implementation, several EMA (CE-marked) and/or Food and Drug Administration (FDA; 510[k])-cleared softwares including the CL metric are (becoming) available (Figure 1, see also Table S1) and the package inserts of the amyloid PET tracers were amended in Europe to include quantification as an adjunct to the visual read (VR). Given its possible wide applicability and inherent generalizability, 159 papers have been published mentioning the CL scale since its first introduction in 2015 (Figure 2).

### 3 | CENTILOID REFLECTS THE DEGREE OF AMYLOID PATHOLOGY

In the clinical routine, information regarding the degree of amyloid pathology is often omitted and reduced to a binary measure based

on PET visual assessment, in line with current FDA and the initial EMA labels of the amyloid PET tracers. A major advantage of quantification is its ability to provide information on the amount of pathology, which could be reflective of different disease stages. In this section, existing CL thresholds established from gold (post mortem) and clinical standards (cerebrospinal fluid [CSF] and VR) are discussed.

#### 3.1 | Centiloid compared to the gold standard (post mortem)

Histopathological studies are the gold standard to establish the presence and amount of amyloid pathology. In most cases, these studies rely on the maximum neuritic plaque density found in specific neocortical areas defined using the Consortium to Establish a Registry for Alzheimer's Disease (CERAD).<sup>20</sup> CERAD classifies neuritic plaque density into four categories: none, sparse, moderate, or frequent. The distinction between none-to-sparse and moderate-to-frequent as being  $A\beta$ -negative or  $A\beta$ -positive by pathology was used in the Phase-III validation studies of the F-18 amyloid tracers.<sup>17-19</sup> Optimal thresholds to differentiate between none and sparse-to-frequent plaques have been suggested as 9.6 CL by Amadoru et al.<sup>10</sup> and 12.2 CL by La Joie et al.<sup>11</sup> Differentiating none-to-sparse versus moderate-to-frequent plaque density resulted in a wider range of optimal CL thresholds, from 12 to 35 CL.<sup>10,11,21-24</sup> A stricter approach focusing on none-to-moderate versus frequent amyloid plaques resulted in a threshold of 32.4 CL.<sup>11</sup> In the same study, La Joie et al.<sup>11</sup> also used Thal phases representing the spatial extent of  $A\beta$  pathology<sup>25</sup> to propose thresholds of 12.0 and 23.5 CL to discriminate phases 0 to 1 versus 2 to 5 and 0 to 2 versus 3 to 5, respectively. Finally, using AD neuropathologic change (ADNC)—a combination of CERAD, Thal phases, and Braak tau stages<sup>26</sup>—La Joie et al.<sup>11</sup> and Amadoru et al.<sup>10</sup> found distinct thresholds (24.4 vs 49.4 CL, respectively) to detect intermediate-to-high versus none-to-low ADNC levels. The relatively high 49.4 CL threshold could be explained by the limited number of subjects with a baseline load between 25 and 50 CL and the fact that "likely AD" required a tau Braak III-IV positivity. Thus, the defined 50 CL cut-off might be more reflective of a level of  $A\beta$  pathology associated with established isocortical tau burden.

Despite variability in thresholds, these results suggest that amyloid pathology can be reliably excluded under 10 CL. In contrast, the cutoff for inclusion of amyloid pathology remains somewhat unclear, as post-mortem data-derived cutoffs fall between 12 and 50 CL, depending on included populations, neuropathological scores investigated, and variable intervals between PET acquisition and date of death. Studies comparing the CL scale to clinical measures provide further insights for ruling in  $A\beta$  pathology.

### 3.2 | Centiloid compared to clinically used reference standards (CSF and visual reads)

In clinical practice, AD pathology is commonly evaluated through VR of amyloid-PET scans or analysis of CSF biomarkers, such as  $A\beta_{42}$ , phosphorylated tau (pTau), and total tau (tTau).

The binary VR methods of the approved amyloid-PET tracers were validated as part of their pivotal histopathology Phase-III studies in end-of-life subjects. Studies using VR as the reference standard have reported a wide range of cutoffs reflecting  $A\beta$ -positivity (17 to 42 CL).<sup>2,13,27-30</sup> This is most likely due to differences in reader experience, particularly regarding the assessment of more challenging scans displaying early amyloid-PET uptake, substantial differences in the populations studied, with the number of preclinical individuals being limited or even absent in most VR studies, and differences in radiotracer kinetics. Nonetheless, most VR-based thresholds were estimated to range between 21 and 26 CL.<sup>10,13,31</sup> Expert readers could assess scans as visually positive down to a level of 17 CL and consistently at 25 CL.<sup>13,15</sup>

Compared to CSF  $A\beta_{42}$ , which is expected to change earlier in the AD continuum, Salvadó et al.<sup>15</sup> proposed a cutoff of 12.1 CL to detect early amyloid abnormalities, which is in high agreement with the previously mentioned neuropathological studies.<sup>10,11</sup> In addition, a second threshold of approximately 30 CL was identified to indicate the presence of established pathology based on pTau, tTau, and their ratio with  $A\beta_{42}$ . Importantly, this cutoff was highly consistent (28.6 to 29.7) across these CSF biomarkers reflective of established AD pathology  $A\beta_{42}$ .

Collectively, these findings indicate that at an individual level, 30 CL is a conservative threshold above which there is a high certainty that a relevant amount of amyloid pathology is established.

### 3.3 | CL in the “intermediate range”

The window between 10 and 30 CL units can be regarded as an “intermediate range,” indicative of an evolving pathology trending towards positivity. In the AMYPAD Diagnostic and Patient Management Study (DPMS) dataset, with participants whose features are consistent with those expected in a memory clinic population,<sup>3</sup> around 10% of participants were in that CL band (Figure 3A). Nonetheless, the percentage of intermediate range participants is substantially higher in preclinical AD populations. For example, the AMYPAD Prognostic and Natural History Study (PNHS) reported 22% of individuals with a CL between 10 and 30 units in their primarily cognitively unimpaired cohort above 50 years of age, which is the current target population of early secondary prevention studies like the AHEAD study (Figure 3B).<sup>32</sup> As such, characterizing the CL intermediate range and its associated risk for future disease progression is key.

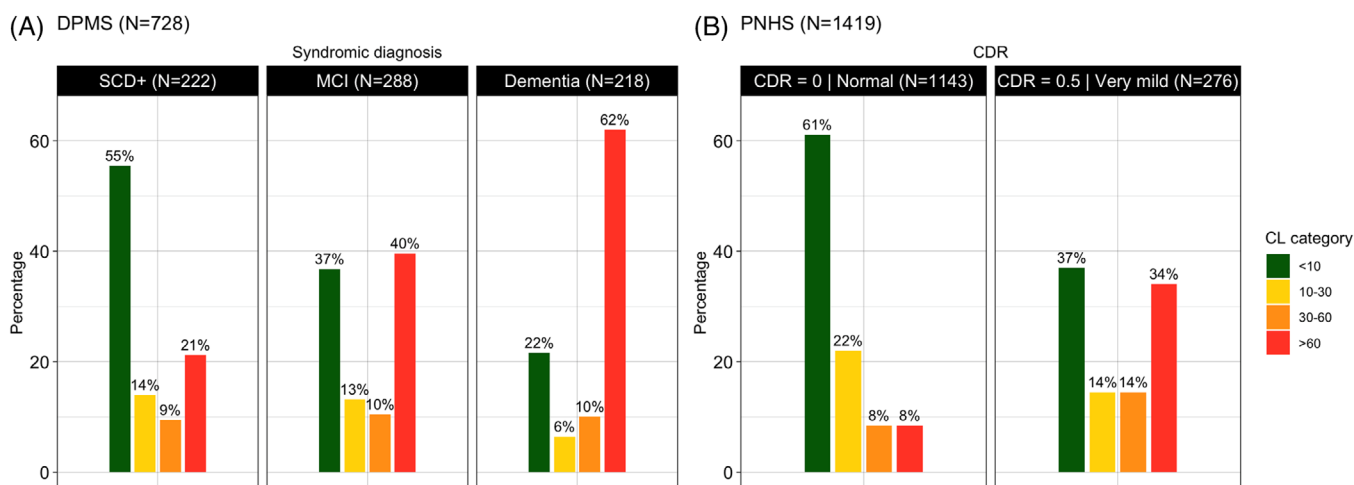


**FIGURE 3** AMYPAD participants categorized by cognitive stage and baseline CL. Bar plots illustrate the distribution of CL groups across two studies, (A) DPMS and (B) PNHS, from the AMYPAD consortium. Subjects were categorized into four groups based on their baseline amyloid burden: <10 CL (no amyloid pathology), 10 to 30 CL (“intermediate range,” evolving amyloid pathology), 30 to 60 CL (established amyloid pathology with increased prevalence of tau positivity), and >60 CL (established amyloid pathology with high certainty of tau-PET positivity). AMYPAD DPMS and PNHS datasets are publicly available (<https://amypad.eu/data/>). AMYPAD, Amyloid Imaging to Prevent Alzheimer’s Disease; CDR, Clinical Dementia Rating; CL, Centiloid; DPMS, Diagnostic and Patient Management Study; MCI, mild cognitive impairment; PNHS, Prognostic and Natural History Study; SCD+, subjective cognitive decline plus.

### 3.3.1 | Centiloid thresholds and disease progression

A growing number of studies have investigated potential cutoffs in the 10 to 30 CL intermediate range to enable the identification of individuals with an increased risk of disease progression. In the earliest stages of AD, Farrell et al. observed an optimal threshold to predict future significant A $\beta$  accumulation ranged from 15 to 17.5 CL in cognitively unimpaired participants across the Australian Imaging, Biomarker and Lifestyle (AIBL), Harvard Aging Brain Study (HABS), and AD Neuroimaging Initiative (ADNI) cohorts.<sup>33</sup> This finding is consistent with the commonly described peak in rate of change before reaching amyloid positivity,<sup>33,34</sup> and with the reliable worsening estimate of 19 CL determined by Jack and colleagues, which reflects the cut point beyond which the amyloid rate of change increases reliably beyond baseline variation in the measure.<sup>35</sup> At the higher end of the intermediate range, a CL of 26 was found to best predict progression to dementia.<sup>27</sup>

Beyond the intermediate range, two studies highlighted a significant rise in the prevalence of tau-PET positivity within the 40 to 70 CL range across ROIs reflecting early to established tau burden.<sup>16,36</sup> Notably, in cognitively unimpaired individuals with CL levels below 50, no tau-PET positivity was observed in the neocortex.<sup>16</sup> Tau-related amyloid levels could be important for patient characterization and selection in future clinical trials. For example, the success of the donanemab TRAILBLAZER-ALZ2 study has been accredited to their participant stratification-based tau burden, selecting specifically those early AD patients that were A $\beta$  positive (CL > 37) and had intermediate tau PET burden.<sup>8</sup> Recently at the Clinical Trials on AD (CTAD) conference, it was demonstrated that this potential high-benefit group could be accurately selected based on CL quantification, with a reported cut point of 60 CL.<sup>37</sup> Taken together, CL provides a tracer-independent measurement of the amount of A $\beta$  pathology. This can be used to stage the disease, to identify those in the early stages who are at risk for progression, and to identify individuals who can benefit the most from disease-modifying treatments. These risk-stratification approaches in combination with other commonly available clinical biomarkers could also support longitudinal monitoring efforts at the individual level, but more studies in such populations and with other outcome measures are needed to further elucidate the CL intermediate range.

## 4 | ROBUSTNESS OF THE CENTILOID SCALE

The AMYPAD consortium was uniquely positioned to assess the robustness of the CL metric due to its multi-site nature and collaborations with the EARL (<https://earl.eanm.org/>), the initiative of the European Association of Nuclear Medicine (EANM), to harmonize quantification in nuclear medicine imaging. To optimally interpret CL values and their associated thresholds, it is critical to consider methodological steps that could impact the precision of the metric. The importance of quantifying PET measurements and their uncertainty have been highlighted in the latest Radiological Society of North America (RSNA) Quantitative Imaging Biomarkers Alliance (QIBA) profile.<sup>38</sup>

The principles in this paper are discussed with respect to the SUVr measure but are equally applicable to the CL measure.

### 4.1 | Sensitivity to pipeline design

While the standard CL pipeline as described by Klunk and colleagues is based on the Statistical Parametric Mapping (SPM), an abundance of alternative pipelines are available.<sup>9</sup> Within the multi-site AMYPAD consortium, the sensitivity of CL quantification to pipeline design, age, atrophy, and image resolution was evaluated by a head-to-head comparison of 32 calibrated CL pipelines covering the typical pipeline design options. In this experiment, four factors were tested: the reference region (RR; whole cerebellum [the primary one], cerebellum grey matter, pons, and cerebellum + brainstem), the analysis space (standard Montreal Neurological Institute [MNI] space vs native space), and definition of target and reference volumes of interest (VOIs; GAAIN VOIs or subject-based segmentations of gray and white matter). Using 533 participants from the AMYPAD-DPMS dataset ( $N_{[18F]flutemetamol} = 207$ ,  $N_{[18F]florbetaben} = 123$ ) and matched individuals from the ADNI database ( $N_{[18F]florbetapir} = 203$ ), generalized estimating equations (GEEs) were used to assess the impact on CL values of the various pipeline design factors.<sup>39</sup> Overall, CL quantification was robust against tracer, and differences in image resolution while using the standard CL pipeline recommended by Klunk et al.<sup>9</sup> Moreover, CL quantification was minimally affected by atrophy in the participants with an average CL of 90, and therefore these differences have no impact on the clinical diagnosis. Importantly, the pons reference region yielded significantly lower CL values as a consequence of age-related white matter uptake, particularly in participants with lower amyloid burden.<sup>40</sup> Within-pipeline 95% confidence intervals ranged from  $\pm 3.3$  to  $\pm 4.0$  CL between 12 and 24 CL, respectively.

### 4.2 | PET-only versus MRI-based pipeline comparison

The need for a magnetic resonance imaging (MRI) scan for CL quantification, as proposed in the original pipeline by Klunk and colleagues, could limit its clinical implementation. Consequently, several PET-only pipelines have been developed, which do not rely on MR for accurate registration.<sup>41,42</sup> For example, the Imaging Dementia—Evidence for Amyloid Scanning (IDEAS) study developed a robust PET-Only Processing (rPOP) pipeline. Thousands of amyloid-PET scans from this study were quantified and similar agreements against VR and the standard CL pipeline were obtained.<sup>41</sup> The AMYPAD consortium performed a head-to-head study, comparing the standard PET-MR pipeline to the AMYPPE PET-only pipeline<sup>43,44</sup> to ensure consistent results regardless of the design. An analysis using 283 [ $^{18}F$ ]flutemetamol scans showed a strong correlation ( $R^2 = 0.97$ ) between the two pipelines and no amyloid burden-dependent systematic bias. There was a low mean absolute deviation ( $5.6 \pm 4.7$  CL) that fell within the noise levels computed in those datasets. Other



PET-only CL pipelines have been implemented with excellent performance against MR-based methods, such as the CapAIBL<sup>45</sup> or the Non-negative Matrix Factorization method.<sup>14</sup>

### 4.3 | Impact of error propagation on Centiloid conversion equations

We also investigated the impact of measurement uncertainty or error propagation in the initial development of the CL conversion equations using a simulation-based design.<sup>46</sup> This was done by adding heteroscedastic Gaussian noise with a larger standard deviation (SD) for higher CL values to 10,000 bootstrap simulations and generating the corresponding CL calibration equation for each simulation. Simulated noise was obtained for each tracer separately and defined as the SD of the error measured in healthy volunteers (0 CL) or AD subjects (100 CL). Simulated noise at intermediate values between 0 and 100 CL was obtained by linear interpolation. A jackknife approach was used to confirm the results obtained from the bootstrap simulations. Overall, in the lower end of the scale, the maximum bias due to error propagation had a small impact on CL measurements (<3.5 CL), while it increased in average up to 8 CL for higher CL values (between 75 and 100 CL). Importantly, the increase in maximum error in the higher range of the scale ( $\approx$ 80 CL) would not have affected classification at the individual level for most of the cutoffs described so far.

### 4.4 | Reliable A $\beta$ accumulation

Assessment of test–retest variability and error propagation of the CL metric is needed to determine what change in CL constitutes a reliable accumulation. The CL metric has been proposed as a useful measure to track amyloid pathology over time and help determine if a subject is accumulating amyloid at a higher pace than healthy elderly individuals. Using data from 1032 participants from the AMYPAD PNHS and Insight46 who underwent [<sup>18</sup>F]flutemetamol, [<sup>18</sup>F]florbetaben, or [<sup>18</sup>F]florbetapir amyloid-PET imaging, a normative strategy was used to define reliable accumulation by estimating the 95th percentile of longitudinal measurements in subpopulations ( $N_{\text{PNHS}} = 101/750$ ,  $N_{\text{Insight46}} = 35/382$ ) expected to remain stable over time. Reliable accumulation was estimated to occur at > 3.0 CL/year.<sup>47</sup> Additional evidence is provided through the placebo groups in recent anti-amyloid trials, which reported rates of amyloid accumulation at a similar magnitude (with baseline amyloid loads between 75 and 101 CL, Figure S1). For example, in the GRADUATE 1 and 2 trials of gantenerumab, the accumulation was approximately 4 CL/year.<sup>5</sup> In the case of aducanumab (high dose), the rates were –0.6 and 2.2 CL/year in the ENGAGE and EMERGE trials, respectively.<sup>4</sup> For lecanemab's Clarity-AD trial, the rate was 2.4 CL/year,<sup>37</sup> while in the donanemab TRAILBLAZER ALZ2 trial (low/medium tau), it was 0.1 CL/year.<sup>8</sup> Following amyloid clearance in the donanemab trial, a re-accumulation rate of 2.8 CL/year was observed.<sup>48</sup>

Of note, in the PNHS, rates of amyloid accumulation from linear mixed-effect models were tracer independent and lower for apolipoprotein E (APOE)  $\epsilon$ 4 noncarriers and for subjects with higher levels of education. Importantly, these results were obtained in a harmonized and curated research cohort. Reliable accumulation at the individual level in real-life clinical settings could be greater.

## 5 | PROPOSED CONTEXT-OF-USE

Taken together, the CL scale provides a valuable approach to attain a standardized and generalizable measure of amyloid burden across tracers and centers. Based on the above, we conclude that CL quantification accurately reflects the amount of AD pathology with a CL value of <10 excluding the presence of any A $\beta$  pathology, while a value of >30 is a conservative estimate of amyloid positivity. Importantly, these proposed cut points reflect the optimal sensitivity and specificity of the metric, respectively, providing high certainty at the individual level (Figure 4). The full distribution of amyloid-positive cut points mentioned can be found in Figure S2. Below we provide specific user guidelines for different scenarios:

### 1. Centiloid quantification is a valuable adjunct to visual assessments of amyloid-PET images to achieve high certainty regarding the presence or absence of A $\beta$ pathology.

This is particularly the case for equivocal scans or for readers with less experience, as recently demonstrated in a prospective study of challenging clinical cases, showing a significant increase in reader agreement and confidence after disclosure of quantitative results.<sup>49</sup> If CL burden is discordant with the visual assessment or falls in between the reliable inclusion and exclusion criteria previously defined (“intermediate range”; in between 10 and 30 CL), readers are encouraged to review the scan for the following signs: focal uptake, brain atrophy, or poor scan quality. Of note, in a clinical setting, individuals with a CL in the intermediate range are a minority (Figure 3A). It is also important to note that both assessment approaches have inherent limitations, as visual reads can be dependent on reader experience, and (CL) quantification is sensitive to deviations in acquisition protocols and processing errors. As such, we recommend the joint use of both assessments to minimize the number of A $\beta$  status misclassifications.

### 2. Anti-amyloid disease modifying therapies: patient inclusion

Drug initiation of anti-amyloid monoclonal antibodies such as lecanemab and donanemab requires high specificity of A $\beta$  status, as serious side effects should only be risked in case of potential treatment benefit. In this context, patients with objective cognitive impairment as determined by a standard neuropsychological evaluation and an abnormal A $\beta$  biomarker could be eligible for these anti-amyloid disease-modifying therapies. An amyloid burden of 30 CL or above could be considered the A $\beta$ -positivity threshold with high certainty (ie, a more conservative threshold) at the individual level. This 30 CL cut point takes into the account

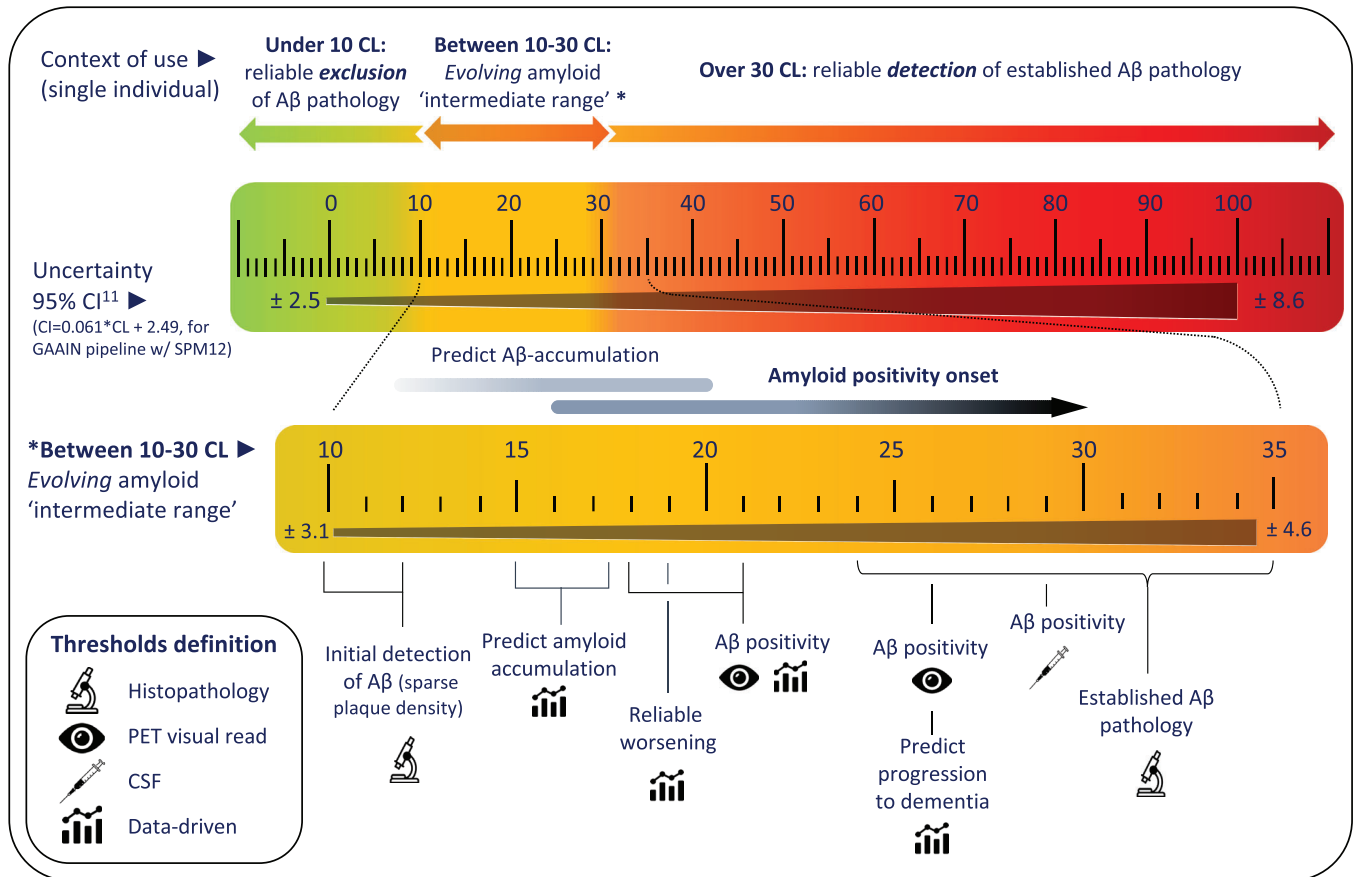


**FIGURE 4** Overview of Centiloid scale interpretation. An illustrative figure summarizing the main studies regarding CL-based cut points to reliability exclude (<10 CL) and include (>30 CL) A $\beta$ -pathology at the individual level. In addition, the 95% confidence interval across the scale is provided and detailed cutoffs in the “intermediate range” are highlighted. A $\beta$ , amyloid-beta; CL, Centiloid; CI, confidence interval; CSF, cerebrospinal fluid; GAAIN, Global Alzheimer’s Association Interactive Network; PET, positron emission tomography; SPM, Statistical Parametric Mapping.

the 95% confidence intervals reflecting the uncertainty in CL quantification.

On the other hand, trials focused on early, primary, or alternative interventions such as changes in lifestyle potentially require optimal sensitivity. As such, the 10 CL threshold (ie, a more liberal threshold) could be implemented to screen out subjects with higher certainty of being A $\beta$ -negative.

3. **The degree of A $\beta$  clearance after treatment with anti-amyloid disease-modifying therapies can be reliably measured with the Centiloid method.**

CL quantification could support significant management changes such as cessation of anti-amyloid therapy once full clearance (ie, amyloid negativity) has been observed.<sup>8,50</sup> Similar criteria could be applied to identify nonresponders after a given treatment period. Relevant to this, anti-amyloid drugs have reported reductions in CL units in the range of 60 to 85 CL, much higher than the uncertainty in CL quantification although treatment cessation decisions might be between 11 and 25 CL<sup>8</sup> and hence the value of knowing the reliability of the CL pipelines at these measures is valuable.

4. **Centiloid quantification could support the identification of early or emerging A $\beta$  pathology, as values that fall within the intermediate range are associated with an increased risk of disease progression.**

Particularly, values above 15 CL have been associated with significant A $\beta$  accumulation towards established A $\beta$  pathology. In addition, reliable accumulation is between 3 and 5 CL per year, depending on the heterogeneity of the cohort, while test-retest and measurement error at the lower end of the scale is between 2.5 and 3.5 CL. Together, CL can be used to include patients in early secondary prevention studies.

## 6 | DEVELOPMENTS AND IMPLEMENTATION

Other clinical applications of the CL scale are currently being investigated. In addition to supporting the detection of amyloid burden and achieving high confidence of A $\beta$  status based on visual assessment, CL quantification could also provide relevant information to support differential diagnosis. A recent study in a mixed memory clinic

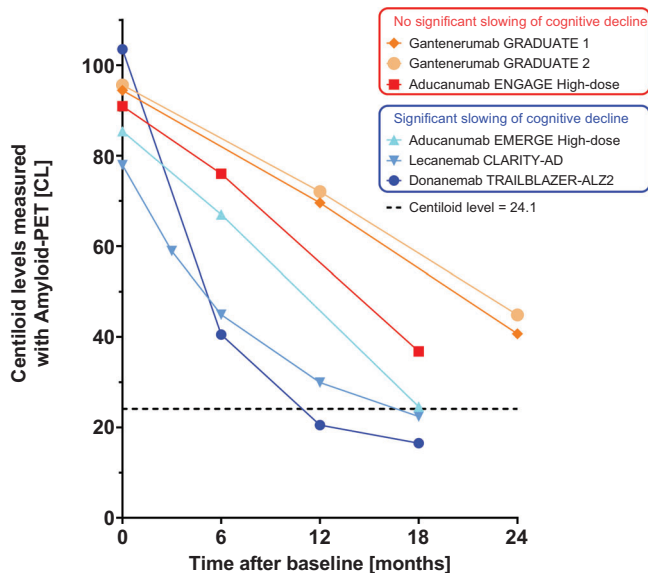


**FIGURE 5** Amyloid- $\beta$  removal profiles for Phase-III trials of aducanumab, donanemab, gantenerumab, and lecanemab as measured by Centiloid (CL). Sample sizes in the treatment arms varied for the individual trials and were at the last visit:  $N = 614$  for donanemab,  $N = 210$  for lecanemab,  $N = 50$  (Graduate 1) and  $N = 41$  (Graduate 2) for gantenerumab, and  $N = 109$  (Emerge high-dose) and  $N = 112$  (Engage high-dose) for aducanumab. Data points as reported in Sims et al. (2023), van Dyck et al. (2022), Bateman et al. (2023), and Budd Haerberlein et al. (2022). Placebo groups are not plotted and showed constant or slightly increasing amyloid levels over time, as expected. The dotted line represents 24.1 CL, the cutoff for amyloid-negativity as defined within the GRADUATE 1 and 2 trials and implemented in the head-to-head studies of donanemab versus Aduhelm.

population illustrated that visual amyloid-positivity was associated with a wide range of CL units across clinical stages. Importantly, CL quantification was associated with the primary etiological diagnosis after correction for the clinical stage, with AD patients displaying the highest amyloid burden, followed by dementia with Lewy bodies and cerebrovascular disease.<sup>2</sup> These results also support the notion that CL levels lower than expected, based on clinical stage, might be indicative of co-pathology rather than the primary etiology underlying cognitive decline.

In the context of clinical trials and future routine implementation, further work is needed to assess how CL values could be used to further improve patient benefit-risk stratification and for monitoring an individual's response to therapy. Recently completed anti-amyloid trials revealed a slowing of cognitive decline if full clearance of amyloid was obtained within 18 months (Figure 5). Determining successful amyloid clearance would allow discontinuation of treatment, reducing patient and facility burden, costs, and potential harmful side effects. The donanemab TRAILBLAZER-ALZ2 Phase-III trial already implemented this approach, switching patients to placebo if one PET scan revealed  $CL < 11$ , or if two consecutive PET scans had amyloid levels in between 11 and 25 CL (amyloid clearance defined at 24.1 CL).<sup>8</sup> After anti- $A\beta$  therapy, CL estimates could also be used to assess potential re-accumulation.<sup>51</sup> In terms of risk stratification, future work is

### Box 1: Centiloid quantification: A powerful tool, not a magic bullet

#### Strengths:

The Centiloid (CL) method:

1. provides a global, semi-quantitative measure of amyloid- $\beta$  burden as measured by positron emission tomography (PET) imaging;
2. improves the interpretability of amyloid-PET values with clinically relevant 0 and 100 anchor points;
3. facilitates dataset sharing and merging across groups using different tracers and/or pipelines;
4. allows comparison of amyloid-PET values across publications and clinical trials.

#### Notes of caution:

1. Similar to standard uptake value ratio (SUVr) values, CLs
  - depend on the quality of image acquisition and processing
  - can be inaccurate in case of atypical amyloid distribution affecting the reference region (eg, the elevated signal in the cerebellum) or the cortex (eg, signal limited to cortical areas outside the mask)
2. Rigorous steps are needed to validate the equation to convert original PET metrics (eg, SUVr) to CLs; equations are tracer/pipeline/acquisition time-window specific.
3. CL transformation harmonizes the dynamic range across tracers, but not measurement error/noise

needed to elucidate to what extent continuous CL burden could be implemented to further inform on individual risk-benefit ratios. For example, results from the donanemab Phase-III trial demonstrate that clinical benefit is reduced in patients with high tau burden (possibly associated with higher CL values; see Figure S3). Additional CL cutoffs could be implemented to estimate an individual's likelihood of tau-PET burden. In addition, results presented at the CTAD 2023 conference suggest that high baseline CL in combination with other risk factors such as homozygous APOE  $\epsilon 4$  carriership, cardiovascular risk factors, and the presence of microbleeds and/or superficial siderosis based on MRI brain imaging, is associated with risk of developing amyloid-related imaging abnormalities (ARIA), the most common side effect of anti-amyloid therapies.<sup>52-54</sup>

Finally, the rapid developments in plasma biomarker assays are revolutionizing the field of patient screening/selection for trials and disease-modifying treatments.<sup>55</sup> Blood-based biomarkers are convenient for predicting amyloid positivity and to a certain extent tau burden.<sup>56</sup> Considering the disease-staging capacities of CL cut points, it is of great interest to determine whether CL could also be used in conjunction with plasma biomarkers to further optimize stratification and support risk-benefit considerations at the individual level.<sup>57</sup>



## 7 | METHODOLOGICAL CONSIDERATIONS AND LIMITATIONS

The application of the CL scale, although a significant advancement in the standardization of amyloid PET quantification, still presents some outstanding challenges. One critical issue is to verify the thresholds across different populations, particularly those that are underrepresented in existing research, such as Black and Hispanic individuals.<sup>58</sup> This is to ensure there are no recruitment biases in clinical and research settings. Thus, further studies in underrepresented populations are required to enhance the generalizability of CL-based assessments.

Moreover, the precision of amyloid measurement is inherently linked to the dynamic range of the tracer used. Evidence suggests that the variance of CL values in young, cognitively normal individuals—expected to be amyloid-negative—is somewhat higher for [<sup>18</sup>F]florbetapir compared to [<sup>18</sup>F]florbetaben and [<sup>18</sup>F]flutemetamol.<sup>1</sup> The effect of tracer on cutoff determination is unknown, as proper head-to-head studies are lacking. Nonetheless, the studies presented in this review cover all three commonly used F18 radiotracers and [<sup>11</sup>C]PiB, and the consistent identification of cut points within the noise range across studies, tracers, and populations suggests that CL mitigates this effect properly. A more specific example comes from the Dominantly Inherited Alzheimer Network study, which showed that PiB and [<sup>18</sup>F]florbetapir differ in their ability to track treatment response using SUVR but not CL, consistent with the intended purpose of the CL method. Therefore, this study shows that the CL scale eliminates between-tracer longitudinal differences even when changes are due to anti-A $\beta$  drug treatment, as opposed to disease progression alone.<sup>59</sup> Future studies should determine the tracer-associated bias of CL and determine whether cut point confidence intervals are tracer-dependent.

In related fashion, CL quantification demonstrates similar results across different tracers at the group level, providing a reliable means of comparing amyloid burden in large-scale studies. However, this apparent consistency could mask underlying discrepancies due to technical factors at the individual level. Further studies could investigate the CL variability across established research pipelines and regulatory-approved software and the impact of clinical decision-making at the single-person level.

Finally, the CL approach provides a robust measure of the extent of amyloid burden due to its standardized target ROI.<sup>9</sup> While this ROI encompasses the main cortical regions showing amyloid-PET uptake, posterior/occipital regions are underrepresented or even excluded. As such, atypical patterns of amyloid-PET signal could be missed using CL quantification,<sup>60,61</sup> further highlighting the importance to utilize quantification in conjunction with visual assessments.<sup>44</sup>

## 8 | CONCLUSION

For the three approved FDA/EMA amyloid-PET radiotracers, the CL scale is a robust, tracer-independent, and validated metric reflecting the degree of amyloid pathology that is suitable to be used in clinical

settings. At the individual level, a CL below 10 reliably excludes amyloid pathology, while a CL above 30 reliably detects abnormal accumulation. Values between these thresholds signify an intermediate range, indicating evolving levels of amyloid. The uncertainty of the CL metric ( $\approx 3$  CL around 10 CL, up to 8 CL around 80 CL) should always be considered when interpreting the amyloid load against established thresholds and in longitudinal evaluations. In the future, CL quantification could be used for benefit–risk stratification, disease monitoring, and patient management. Notably, the use of amyloid-PET quantification in the clinical routine as adjunct to the visual assessment is currently approved in Europe by the EMA and Medicines and Healthcare Products Regulatory Agency (MHRA). In the US, the FDA-approved method for PET scan assessment is still based on VR only. This perspective review provides further evidence for its utility and global implementation.

### ACKNOWLEDGMENTS

The project leading to this paper has received funding from the Innovative Medicines Initiative 2 Joint Undertaking under grant agreement No. 115952. This joint undertaking receives the support from the European Union's Horizon 2020 research and innovation program and EFPIA. This communication reflects the views of the authors and neither IMI nor the European Union and EFPIA are liable for any use that may be made of the information contained herein.

### CONFLICT OF INTERESTS STATEMENT

Ariane Bollack is employed by GE HealthCare. Alexander Drzezga has received research support from Siemens Healthineers, Life Molecular Imaging, GE Healthcare, AVID Radiopharmaceuticals, Sofie, Eisai, Novartis/AAA, and Ariceum Therapeutics; has served as Speaker Honorary/Advisory Boards for Siemens Healthineers, Sanofi, GE Healthcare, Biogen, Novo Nordisk, Invicro, Novartis/AAA, and Bayer Vital; holds stock in Siemens Healthineers, Lantheus Holdings, Structured therapeutics, and ImmunoGen; and holds a patent for 18F-JK-PSMA-7 (Patent No.: EP3765097A1; Date of patent: Jan 20, 2021). Aleksandar Jovalekic is employed by Life Molecular Imaging. Andrew W. Stephens is employed by Life Molecular Imaging. Christopher Buckley is employed by GE HealthCare. David Valléz Garcíá has no relevant disclosures. Frederik Barkhof is supported by the NIHR biomedical research center at UCLH; serves as a steering committee or Data Safety Monitoring Board member for Biogen, Merck, Eisai, and Prothena; serves as an advisory board member for Combinostics and Scottish Brain Sciences; serves as a consultant for Roche, Celltrion, Rewind Therapeutics, Merck, and Bracco; has research agreements with ADDI, Merck, Biogen, GE Healthcare, and Roche; and is co-founder and shareholder of Queen Square Analytics LTD. Gill Farrar is employed by GE HealthCare. Juan Domingo Gispert has received research support from GE HealthCare, Roche Diagnostics, and Hoffmann – La Roche; has received speaker/consulting fees from Roche Diagnostics, Philips Nederlands, Esteve, Biogen, and Life Molecular Imaging; and serves in the Molecular Neuroimaging Advisory Board of Prothena Biosciences. Lyduine E. Collij has received research support from GE Healthcare and Springer Healthcare (funded by Eli Lilly),

both paid to the institution; Dr. Collij's salary is supported by an MSCA postdoctoral fellowship research grant (#101108819) and an Alzheimer Association Research Fellowship (AARF) grant (#23AARF-1029663). Mark Battle is employed by GE HealthCare. Mahnaz Shekari has no relevant disclosures. Norman Koglin is employed by Life Molecular Imaging. Núria Roé-Vellvé is employed by Life Molecular Imaging. Santiago Bullich is employed by Life Molecular Imaging. Renaud La Joie receives funding from NIH/NIA (P30-AGO62422, K99AG065501), the US Department of Defense, and the Alzheimer's Association (AARG-22-926899); and is an associate editor for *Alzheimer's Research & Therapy*. Valentina Garibotto is supported by the Swiss national science foundation (project n.320030\_185028 and 320030\_169876), the Aetas Foundation, the Schmidheiny Foundation, the Velux Foundation, the Fondation privée des HUG; and has received support for research and speakers' fees from Siemens Healthineers, GE HealthCare, Janssen, and Novo Nordisk, all paid to the institution. Author disclosures are available in the [Supporting information](#).

## ORCID

Lyduine E. Collij  <https://orcid.org/0000-0001-6263-1762>  
 Ariane Bollack  <https://orcid.org/0000-0002-9169-7530>  
 Renaud La Joie  <https://orcid.org/0000-0003-2581-8100>  
 Mahnaz Shekari  <https://orcid.org/0000-0003-1336-6768>  
 Norman Koglin  <https://orcid.org/0000-0001-7583-8201>  
 David Valléz Garcá  <https://orcid.org/0000-0003-3308-3167>  
 Valentina Garibotto  <https://orcid.org/0000-0003-2422-698X>  
 Andrew W. Stephens  <https://orcid.org/0000-0001-5052-6586>  
 Frederik Barkhof  <https://orcid.org/0000-0003-3543-3706>  
 Juan Domingo Gispert  <https://orcid.org/0000-0002-6155-0642>

## REFERENCES

- Pemberton HG, Collij LE, Heeman F, et al. Quantification of amyloid PET for future clinical use: a state-of-the-art review. *Eur J Nucl Med Mol Imaging*. 2022;49(10):3508-3528. doi:10.1007/s00259-022-05784-y
- Collij LE, Salvadó G, de Wilde A, et al. Quantification of [18F]florbetaben amyloid-PET imaging in a mixed memory clinic population: the ABIDE project. *Alzheimers Dement*. 2023;19(6):2397-2407. doi:10.1002/alz.12886
- Altomare D, Collij L, Caprioglio C, et al. Description of a European memory clinic cohort undergoing amyloid-PET: the AMY-PAD Diagnostic and Patient Management Study. *Alzheimers Dement*. 2023;19(3):844-856. doi:10.1002/alz.12696
- Budd Haerberlein S, Aisen PS, Barkhof F, et al. Two randomized phase 3 studies of aducanumab in early Alzheimer's disease. *J Prev Alzheimers Dis*. 2022;9(2):197-210. doi:10.14283/jpad.2022.30
- Bateman RJ, Smith J, Donohue MC, et al. Two phase 3 trials of gantenerumab in early Alzheimer's disease. *N Engl J Med*. 2023;389(20):1862-1876. doi:10.1056/NEJMoa2304430
- van Dyck CH, Swanson CJ, Aisen P, et al. Lecanemab in early Alzheimer's disease. *N Engl J Med*. 2023;388(1):9-21. doi:10.1056/NEJMoa2212948
- Cummings J, Apostolova L, Rabinovici GD, et al. Lecanemab: appropriate use recommendations. *J Prev Alzheimers Dis*. 2023;10(3):362-377. doi:10.14283/jpad.2023.30
- Sims JR, Zimmer JA, Evans CD, et al. Donanemab in early symptomatic Alzheimer disease: the TRAILBLAZER-ALZ 2 randomized clinical trial. *JAMA*. 2023;330(6):512-527. Published online July 17. doi:10.1001/jama.2023.13239
- Klunk WE, Koeppe RA, Price JC, et al. The Centiloid project: standardizing quantitative amyloid plaque estimation by PET. *Alzheimers Dement J Alzheimers Assoc*. 2015;11(1):1-15.e4. doi:10.1016/j.jalz.2014.07.003
- Amadoru S, Doré V, McLean CA, et al. Comparison of amyloid PET measured in Centiloid units with neuropathological findings in Alzheimer's disease. *Alzheimers Res Ther*. 2020;12(1):22. doi:10.1186/s13195-020-00587-5
- La Joie R, Ayakta N, Seeley WW, et al. Multisite study of the relationships between *antemortem* [<sup>11</sup>C]PIB-PET Centiloid values and *postmortem* measures of Alzheimer's disease neuropathology. *Alzheimers Dement*. 2019;15(2):205-216. doi:10.1016/j.jalz.2018.09.001
- Reinartz M, Luckett ES, Schaevebeke J, et al. Classification of 18F-Flutemetamol scans in cognitively normal older adults using machine learning trained with neuropathology as ground truth. *Eur J Nucl Med Mol Imaging*. 2022;49(11):3772-3786. doi:10.1007/s00259-022-05808-7
- Collij LE, Salvadó G, Shekari M, et al. Visual assessment of [18F]flutemetamol PET images can detect early amyloid pathology and grade its extent. *Eur J Nucl Med Mol Imaging*. 2021;48(7):2169-2182. doi:10.1007/s00259-020-05174-2
- Bourgeat P, Doré V, Doecke J, et al. Non-negative matrix factorisation improves Centiloid robustness in longitudinal studies. *NeuroImage*. 2021;226:117593. doi:10.1016/j.neuroimage.2020.117593
- Salvadó G, Molinuevo JL, Brugulat-Serrat A, et al. Centiloid cut-off values for optimal agreement between PET and CSF core AD biomarkers. *Alzheimers Res Ther*. 2019;11(1):27. doi:10.1186/s13195-019-0478-z
- Doré V, Krishnadas N, Bourgeat P, et al. Relationship between amyloid and tau levels and its impact on tau spreading. *Eur J Nucl Med Mol Imaging*. 2021;48(7):2225-2232. doi:10.1007/s00259-021-05191-9
- Clark CM, Schneider JA, Bedell BJ, et al. Use of Florbetapir-PET for Imaging  $\beta$ -Amyloid Pathology. *JAMA*. 2011;305(3):275-283. doi:10.1001/jama.2010.2008
- Sabri O, Sabbagh MN, Seibyl J, et al. Florbetaben PET imaging to detect amyloid beta plaques in Alzheimer's disease: phase 3 study. *Alzheimers Dement J Alzheimers Assoc*. 2015;11(8):964-974. doi:10.1016/j.jalz.2015.02.004
- Curtis C, Gamez JE, Singh U, et al. Phase 3 trial of flutemetamol labeled with radioactive fluorine 18 imaging and neuritic plaque density. *JAMA Neurol*. 2015;72(3):287-294. doi:10.1001/jamaneurol.2014.4144
- Mirra SS, Heyman A, McKeel D, et al. The Consortium to Establish a Registry for Alzheimer's Disease (CERAD): Part II. Standardization of the neuropathologic assessment of Alzheimer's disease. *Neurology*. 1991;41(4):479-479. doi:10.1212/WNL.41.4.479
- Jovalekic A, Roé-Vellvé N, Koglin N, et al. Validation of quantitative assessment of florbetaben PET scans as an adjunct to the visual assessment across 15 software methods. *Eur J Nucl Med Mol Imaging*. 2023;50(11):3276-3289. doi:10.1007/s00259-023-06279-0
- Doré V, Bullich S, Rowe CC, et al. Comparison of 18F-florbetaben quantification results using the standard Centiloid, MR-based, and MR-less CapAIBL® approaches: validation against histopathology. *Alzheimers Dement J Alzheimers Assoc*. 2019;15(6):807-816. doi:10.1016/j.jalz.2019.02.005
- Clark CM, Pontecorvo MJ, Beach TG, et al. Cerebral PET with florbetapir compared with neuropathology at autopsy for detection of neuritic amyloid- $\beta$  plaques: a prospective cohort study. *Lancet Neurol*. 2012;11(8):669-678. doi:10.1016/S1474-4422(12)70142-4
- Navitsky M, Joshi AD, Kennedy I, et al. Standardization of amyloid quantitation with florbetapir standardized uptake value ratios to the Centiloid scale. *Alzheimers Dement*. 2018;14(12):1565-1571. doi:10.1016/j.jalz.2018.06.1353
- Thal DR, Rüb U, Orantes M, Braak H. Phases of A $\beta$ -deposition in the human brain and its relevance for the development of AD. *Neurology*. 2002;58(12):1791-1800. doi:10.1212/WNL.58.12.1791

26. Hyman BT, Phelps CH, Beach TG, et al. National Institute on Aging – Alzheimer's Association guidelines for the neuropathologic assessment of Alzheimer's disease. *Alzheimers Dement*. 2012;8(1):1-13. doi:10.1016/j.jalz.2011.10.007
27. Hanseeuw BJ, Malotau V, Dricot L, et al. Defining a Centiloid scale threshold predicting long-term progression to dementia in patients attending the memory clinic: an [18F] flutemetamol amyloid PET study. *Eur J Nucl Med Mol Imaging*. 2021;48(1):302-310. doi:10.1007/s00259-020-04942-4
28. Battle M, Buckley C, Smith A, et al. Comparison of Centiloid scaling values with visual read assessment in a pathology verified autopsy cohort. *Eur J Nucl Med Mol Imaging*. 2019;46:S322-S323. Springer Verlag. Accessed December 21, 2023. <https://lirias.kuleuven.be/2901564>
29. Bullich S, Roé-Vellvé N, Marquié M, et al. Early detection of amyloid load using 18F-florbetaben PET. *Alzheimers Res Ther*. 2021;13:67. doi:10.1186/s13195-021-00807-6
30. Roysse SK, Minhas DS, Lopresti BJ, et al. Validation of amyloid PET positivity thresholds in Centiloids: a multisite PET study approach. *Alzheimers Res Ther*. 2021;13(1):99. doi:10.1186/s13195-021-00836-1
31. Collij LE, Salvadó G, de Wilde A, et al. Quantification of [18F]florbetaben amyloid-PET imaging in a mixed memory clinic population: the ABIDE project. *Alzheimers Dement*. 2022;19(6):2397-2407. doi:10.1002/alz.12886
32. Rafii MS, Sperling RA, Donohue MC, et al. The AHEAD 3-45 Study: design of a prevention trial for Alzheimer's disease. *Alzheimers Dement*. 2022;19(4):1227-1233. doi:10.1002/alz.12748
33. Farrell M. Defining the lowest threshold for amyloid-PET to predict future cognitive decline and amyloid accumulation | neurology. *Neurology*. 2021;96(4):e619-e631. doi:10.1212/WNL.00000000000011214
34. Betthausen TJ, Kosciak RL, Jedynak BM, et al. Multi-method investigation of factors influencing amyloid onset and impairment in three cohorts. *Brain*. 2022;145(11):4065-4079.
35. Jack CR, Wiste HJ, Weigand SD, et al. Defining imaging biomarker cut points for brain aging and Alzheimer's disease. *Alzheimers Dement*. 2017;13(3):205-216. doi:10.1016/j.jalz.2016.08.005
36. Bullich S, Mueller A, De Santi S, et al. Evaluation of tau deposition using 18F-PI-2620 PET in MCI and early AD subjects—a MissionAD tau sub-study. *Alzheimers Res Ther*. 2022;14(1):105. doi:10.1186/s13195-022-01048-x
37. van Dyck C, Sperling R, Li D, et al. Lecanemab for the Treatment of Early Alzheimer's Disease: The Extension of Efficacy Results from Clarity AD. Presented at: CTAD; 2022. [https://www.eisaimedicalinformation.com/-/media/Files/EisaiMedicalInformation/Neurology/Congress-Materials/ADPD-2024/vanDyck\\_ADPD2024\\_3\\_9\\_24\\_cvd.pdf?hash=108ef6e4-90dd-4eed-8418-3dabd0866bd5](https://www.eisaimedicalinformation.com/-/media/Files/EisaiMedicalInformation/Neurology/Congress-Materials/ADPD-2024/vanDyck_ADPD2024_3_9_24_cvd.pdf?hash=108ef6e4-90dd-4eed-8418-3dabd0866bd5)
38. Smith AM, Obuchowski NA, Foster NL, et al. The RSNA QIBA profile for amyloid pet as an imaging biomarker for cerebral amyloid quantification. *J Nucl Med*. 2023;64(2):294-303. doi:10.2967/jnumed.122.264031
39. Shekari M, Váñez García D, Collij LE, et al. Stress testing the Centiloid: precision and variability of PET quantification of amyloid pathology. *Alzheimers Dement*. 2024;20(8):5102-5113. doi:10.1002/alz.13883
40. Shekari M, Salvadó G, Battle MR, et al. Evaluating robustness of the Centiloid scale against variations in amyloid PET image resolution. *Alzheimers Dement*. 2021;17(S1):e055726. doi:10.1002/alz.055726
41. Iaccarino L, La Joie R, Koeppe R, et al. rPOP: robust PET-only processing of community acquired heterogeneous amyloid-PET data. *NeuroImage*. 2022;246:118775. doi:10.1016/j.neuroimage.2021.118775
42. Doré V, Bullich S, Rowe CC, et al. Comparison of <sup>18</sup>F-florbetaben quantification results using the standard Centiloid, MR-based, and MR-less CapAIBL® approaches: validation against histopathology. *Alzheimers Dement*. 2019;15(6):807-816. doi:10.1016/j.jalz.2019.02.005
43. Amytype. <https://gehealthcare.box.com/s/2tfq61oz8vlyvycx16x0Yl8s24hk4nf>
44. Collij LE, Bischof GN, Altomare D, et al. Quantification supports amyloid-PET visual assessment of challenging cases: results from the AMYPAD-DPMS study. Published online May 22, 2024. doi:10.1101/2024.05.22.24307653
45. Bourgeat P, Doré V, Fripp J, et al. Implementing the Centiloid transformation for 11C-PiB and  $\beta$ -amyloid 18F-PET tracers using CapAIBL. *NeuroImage*. 2018;183:387-393. doi:10.1016/j.neuroimage.2018.08.044
46. Roé-Vellvé N, Farrar G, Collij L, et al. Impact of error propagation in the development of the Centiloid conversion equation. *Eur J Nucl Med Mol Imaging*. 2022;49(1):S548.
47. Bollack A, Collij LE, García DV, et al. Investigating reliable amyloid accumulation in Centiloids: results from the AMYPAD Prognostic and Natural History Study. *Alzheimers Dement*. 2024;20(5):3429-3441. doi:10.1002/alz.13761
48. Eli L. Insights from TRAILBLAZER-ALZ 2 (Donanemab): Potential Clinical Translation. Published online 2024. [https://assets.ctfassets.net/mpejy6umgthp/4Xzve6Up2kj9uvvfkAJ3D/c9dfd30ccc0a449c80b35ef761e5fe41/VV-DONPT3\\_AAIC2024\\_ZIMMER\\_TRLBL\\_ALZ-2\\_INSIGHTS\\_DV-024669\\_V7.4.pdf](https://assets.ctfassets.net/mpejy6umgthp/4Xzve6Up2kj9uvvfkAJ3D/c9dfd30ccc0a449c80b35ef761e5fe41/VV-DONPT3_AAIC2024_ZIMMER_TRLBL_ALZ-2_INSIGHTS_DV-024669_V7.4.pdf)
49. Collij LE, Bischof GN, Altomare D, et al. Quantification supports visual assessment of challenging amyloid-PET images. *Alzheimers Dement*. 2023;19(S17):e074620. doi:10.1002/alz.074620
50. Jack Jr CR, Andrews JS, Beach TG, et al. Revised criteria for diagnosis and staging of Alzheimer's disease: Alzheimer's Association Workgroup. *Alzheimers Dement*. 2024;20(8):5143-5169. doi:10.1002/alz.13859
51. Shcherbinin S, Evans CD, Lu M, et al. Association of amyloid reduction after donanemab treatment with tau pathology and clinical outcomes: the TRAILBLAZER-ALZ randomized clinical trial. *JAMA Neurol*. 2022;79(10):1015-1024. doi:10.1001/jamaneurol.2022.2793
52. Swanson CJ, Zhang Y, Dhadda S, et al. A randomized, double-blind, phase 2b proof-of-concept clinical trial in early Alzheimer's disease with lecanemab, an anti-A $\beta$  protofibril antibody. *Alzheimers Res Ther*. 2021;13(1):80. doi:10.1186/s13195-021-00813-8
53. Mintun MA, Lo AC, Duggan Evans C, et al. Donanemab in Early Alzheimer's Disease. *N Engl J Med*. 2021;384(18):1691-1704. doi:10.1056/NEJMoa2100708
54. Salloway S, Chalkias S, Barkhof F, et al. Amyloid-related imaging abnormalities in 2 phase 3 studies evaluating aducanumab in patients with early Alzheimer disease. *JAMA Neurol*. 2022;79(1):13-21.
55. Hansson O, Blennow K, Zetterberg H, Dage J. Blood biomarkers for Alzheimer's disease in clinical practice and trials. *Nat Aging*. 2023;3(5):506-519. doi:10.1038/s43587-023-00403-3
56. Mattsson-Carlsson N, Collij LE, Stomrud E, et al. Plasma biomarker strategy for selecting patients with Alzheimer disease for anti-amyloid immunotherapies. *JAMA Neurol*. 2024;81(1):69-78. doi:10.1001/jamaneurol.2023.4596
57. Ashton NJ, Janelidze S, Mattsson-Carlsson N, et al. Differential roles of A $\beta$ 42/40, p-tau231 and p-tau217 for Alzheimer's trial selection and disease monitoring. *Nat Med*. 2022;28(12):2555-2562. doi:10.1038/s41591-022-02074-w
58. Reardon S. Alzheimer's drug trials plagued by lack of racial diversity. *Nature*. 2023;620(7973):256-257. doi:10.1038/d41586-023-02464-1

59. Chen CD, McCullough A, Gordon B, et al. Longitudinal head-to-head comparison of 11C-PiB and 18F-florbetapir PET in a Phase 2/3 clinical trial of anti-amyloid- $\beta$  monoclonal antibodies in dominantly inherited Alzheimer's disease. *Eur J Nucl Med Mol Imaging*. 2023;50(9):2669-2682. doi:10.1007/s00259-023-06209-0
60. Collij LE, Salvadó G, Wottschel V, et al. Spatial-temporal patterns of  $\beta$ -amyloid accumulation. *Neurology*. 2022;98(17):e1692-e1703. doi:10.1212/WNL.0000000000200148
61. Charidimou A, Farid K, Tsai HH, Tsai LK, Yen RF, Baron JC. Amyloid-PET burden and regional distribution in cerebral amyloid angiopathy: a systematic review and meta-analysis of biomarker performance. *J Neurol Neurosurg Psychiatry*. 2018;89(4):410-417. doi:10.1136/jnnp-2017-316851

## SUPPORTING INFORMATION

Additional supporting information can be found online in the Supporting Information section at the end of this article.

**How to cite this article:** Collij LE, Bollack A, La Joie R, et al. Centiloid recommendations for clinical context-of-use from the AMYPAD consortium. *Alzheimer's Dement*. 2024;1-12. <https://doi.org/10.1002/alz.14336>